Probing the Warm Gas in Alignment Effect Radio Galaxies

Mark J. Neeser[1], Hans Hippelein[2], and Klaus Meisenheimer[2]

[1] Kapteyn Astronomical Institute, Postbus 800, NL-9700 AV Groningen, The Netherlands

[2] Max-Planck-Institut für Astronomie, Königstuhl 17, 69117 Heidelberg, Germany

Abstract

We report on the results of a three-dimensional investigation of the extended line-emission in 11 3CR radio galaxies ($0.5 < z < 1.1$). Using a Fabry-Perot etalon to obtain both the kinematics and morphology of the [O II]λ3727 gas, our goal was to find the mechanisms responsible for the creation and excitation of this warm gas, and the source of its alignment with the radio emission.

1 Introduction

Powerful radio galaxies are often associated with complex extended emission-line regions that can have linear sizes of up to several hundred kpc. The first systematic imaging surveys by McCarthy et al. (1987) and Baum et al. (1988) (high and low z 3CR sources, respectively), and by Chambers et al. (1987) (4C sources) revealed a tendency for the extended gas in many radio galaxies to share the same axis as that of the double-lobed radio emission. Furthermore, the fraction of radio galaxies displaying this emission-line *alignment effect* rapidly changes from a few at low redshifts, to nearly all for $z > 0.3$.

The novelty of the alignment effect, combined with the often spectacular morphologies of extended emission-line regions and their potential effects on the formation and evolution of radio galaxies, attracted lively debate, little consensus, and a large number of possible explanations for this phenomenon. The importance of understanding the alignment effect cannot be understated, since the line-emission regions in high redshift radio galaxies, by virtue of their

large intrinsic luminosities and large spatial extents, provide one of the best methods of probing the warm gas at early epochs. Since this phenomena arises in extended, highly dynamic gas, an investigation that combines well-resolved morphologies with kinematics would go far in shedding new light on the origin of the line-emission gas and its source of excitation. As such, we began a detailed study of the morphologies, velocities, and line widths of these galaxies. The specific questions that we wanted to answer concerned the three-dimensional structure of the [O II] gas and its association with the radio galaxy, the motion of this gas with respect to the central source, and the mechanisms by which the line-emission regions are excited. By addressing these issues we attempted to find the source of the warm gas alignment in each of our radio galaxies.

2 Observational Methods

Selecting the most extended emission-line sources with $z \gtrsim 0.5$ from McCarthy et al. (1995), we imaged a subsample of 3CR radio sources (see Table 1) using a Fabry-Perot (FP) interferometer with spectral and spatial resolutions of 400 km s^{-1} and $\lesssim$ 1.″6, respectively. The etalon was used as a tunable filter and placed in the parallel beam of the focal reducer at the prime focus of the 3.5 m Calar Alto telescope. By stepping the FP along the [O II]λ3727 emission-line (at typically 8–10 wavelength settings across the line), we were able to simultaneously build up a map of the velocity field and image the morphology of the ionized gas. This created a representative sample of 11 radio galaxies observed with unprecedented detail. To investigate the continuum morphology, as well as subtract its contribution to the line-emission images, intermediate-band ($\lambda/\Delta\lambda \simeq 40$) line-free exposures were also obtained on each side of the redshifted [O II]λ3727 line.

3 Main Results From [O II] Sample

Defined by the mechanisms which best explain the excitation, morphology, and kinematics of the warm gas, we find three distinct classes of extended emission-line regions. The physical characteristics of each class are sufficiently unique that they can be used to match a radio galaxy with the mechanism that dominates its line-emission region, despite the fact that some of our sources are sufficiently complex that multiple models for exciting the warm gas are necessary. The

Table 1. Fabry-Perot [O II] Sample

Source	Redshift	[O II] Extent	ΔPA*
3C 34	0.69	17"	18°
3C 44	0.66	10"	27°
3C 54	0.83	5"	15°
3C 124	1.08	4"	7°
3C 169.1	0.63	8"	5°
3C 265	0.81	35"	14°
3C 337	0.64	13"	34°
3C 352	0.81	12"	19°
3C 368	1.13	9"	2°
3C 435A	0.47	16"	11°
3C 441	0.71	5"	22°

*$\Delta PA = |PA_{radio} - PA_{line}|$

archetype source of each class is shown in bold type.

Class 1: Strong galaxy–galaxy interactions.

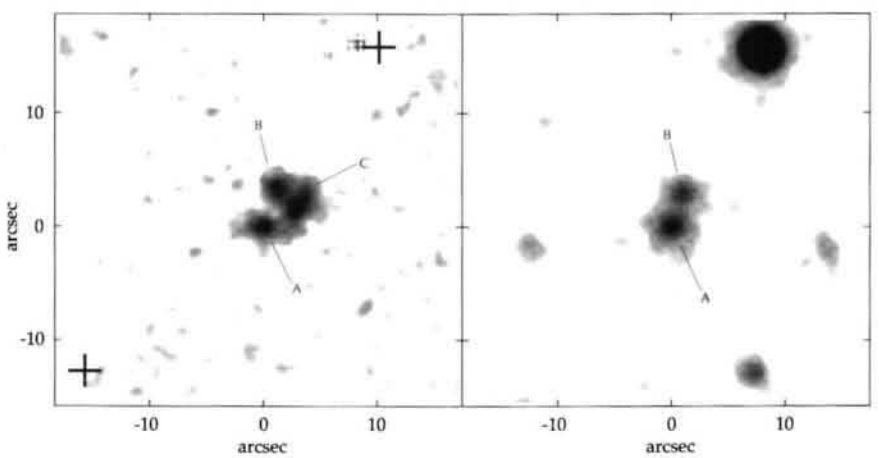

Figure 1. The [O II]λ3727 (left panel) and line-free continuum image (right panel) of 3C 169.1. The radio galaxy (A), its similarly redshifted companion (B), and the gas stripped from it during the interaction (C) are indicated. The radio hotspots are shown with crosses.

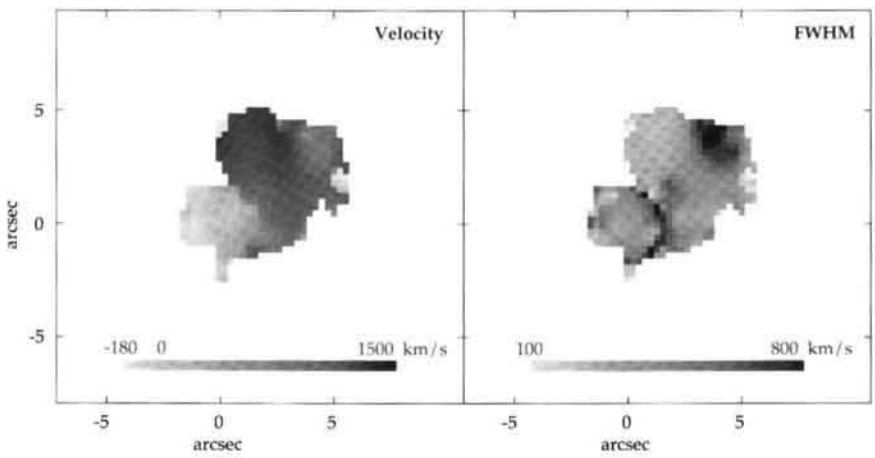

Figure 2. A grayscale representation of the radial velocities (left panel) and the deconvolved line widths (right panel) of the [O II] emission in 3C 169.1. The radio galaxy defines the positional and kinematical origin.

For these radio galaxies we are able to show that the popularly accepted models for exciting the line-emission regions are inadequate to explain all of the observed [O II] features. Instead, we propose a new model in which a close, strong interaction with a companion galaxy exchanges material with the central radio galaxy, creating a complex morphology of bridges, tails and extended knots along the interaction axis. The passage of the companion through the halo of the host source shock–heats the supplied gas and the ambient medium, thus creating part or all of the observed emission-line region and its complex velocity structure. The interaction itself may also be responsible for triggering the radio source of the central galaxy. The sources whose line-emission regions are dominated by this process show one-sided line-emission morphologies distinguished by multiple components, [O II] bridges, and extended linear features (tidal tails). A large range of line-emission sizes and degree of alignments, as well as complex velocity structures are among the features typical of these objects. The intrinsically one-sided nature of the interaction model provides a natural explanation for the very large line-emission brightness, morphology, and velocity asymmetries that define this class (*e.g.* **3C 169.1**, 3C 435A, 3C 44, and the central region of 3C 265).

In the specific case of 3C 169.1 we are probably seeing a close, highly inclined ($\sim$50° into the plane of the sky) passage of a companion galaxy through the high

pressure, low density halo of the radio galaxy. Due to the high relative velocity of this interaction ($\Delta v = 1250\,\mathrm{km\,s^{-1}}$), the ram pressure of the halo will greatly exceed the pressure of the companion's intrinsic gaseous medium. This results in a flattening of the gas, perpendicular to the direction of travel, as it is stripped from the companion at the interaction interface. The gas is shock excited at this position (C), but requires about 10^8 years before its densest parts have sufficiently cooled to emit in the [O II] line. By this time the companion has moved to its current position at B. Both the bridge of line-emission connecting C with the radio galaxy and the velocity gradient along this feature, indicate a mass infall toward the central potential (Neeser et al. 1998).

Since this new model applies to a significant fraction of our radio source sample (~40%), it is important to explain how galaxy–galaxy interactions (an intrinsically geometrically random phenomena) can give rise to alignments between the radio emission and the warm gas. It is plausible that galaxies undergoing gravitational interactions, if aligned with their radio sources, will be preferentially selected by the 3CR catalogue. Most models of double radio sources predict that the radio luminosity of a source will be increased if it expands into a denser gaseous medium (see Eales 1992 for a discussion of this effect). Therefore, since only radio galaxies in which one lobe lies near to the line-emission gas supplied by the companion galaxy will experience an enhancement in radio emission, flux-limited samples will preferentially contain aligned interaction galaxies. The fact that our sources consistently have their brighter and/or closer radio lobe on the same side of the central source as most of their line-emission gas, supports this scenario. Another important clue lies in the fact that all of the interaction galaxies are near to the flux-limit of the 3CR catalogue. This implies that without the radio brightness asymmetries these objects would not have been detected by this survey. By relating the typical radio lobe size and luminosity asymmetries to density differences, we are also able to show that only modest density contrasts ($\frac{\rho_{[\mathrm{OII}]\mathrm{gas}}}{\rho_{\mathrm{IGM}}} \lesssim 7$)—between a radio lobe expanding near to the line-emission gas and its counter part expanding into the ambient intergalactic medium on the other side of the central galaxy—are necessary.

Class 2: Photoionization by a central active galaxy.

For these sources the excitation of the line-emitting gas arises from UV radiation escaping anisotropically from an AGN, hidden from our view by an obscuring torus. In our sample these objects are among the largest and most symmetric sources and are characterized by conical, or bi-conical line-emission structures, complex, often discontinuous velocity structures, and relatively quiescent line

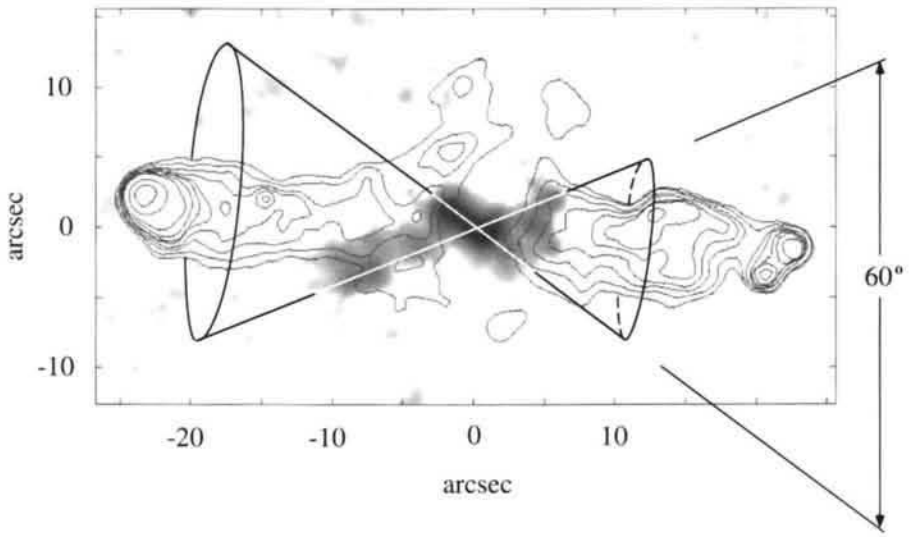

Figure 3. Our proposed photoionization cone superimposed on the grayscale [O II] image of 3C 34. The 20 cm radio map of Neff et al. (1995) is shown as contours. The apex of the cone is located at the position of the central continuum source (the location of the hidden AGN). An opening angle of 60° is the minimum required to photoionize the observed line-emission.

widths (*e.g.* **3C 34** and 3C 265).

The excitation of 3C 34's 120 kpc-sized ($H_o = 50\,km\,s^{-1}\,Mpc^{-1}$, $q_o = 0.5$) [O II] region is best described in terms of photoionizing radiation illuminating the ambient cluster medium of this source (a more detailed account of 3C 34 can be found in Neeser et al. 1997). This is indicated by the distinctively bi-conical morphology of the warm gas in 3C 34. By placing the apex of a symmetrical bi-cone at the position of the central continuum source, we find that we can connect 6 distinct line-emission knots/extensions on both sides of the source, and symmetrically straddle the radio source axis (see Figure 3).

A simple photoionization model shows that this interpretation is energetically viable on these length scales, as long as the cumulative covering factors from the central source to the outermost line-emission components approach unity. The luminosity of the hidden central AGN, necessary to account for the

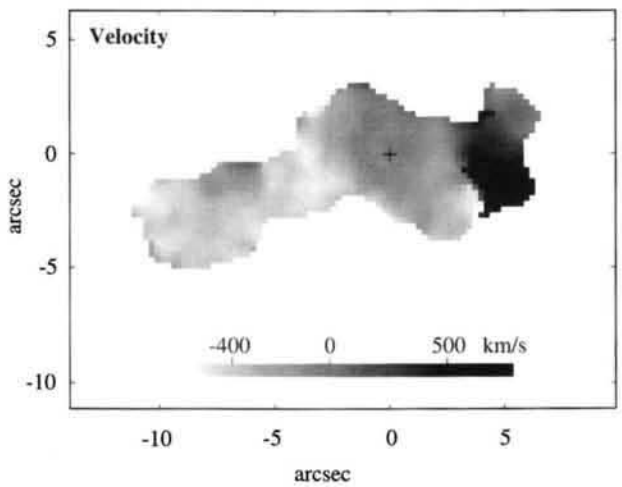

Figure 4. A grayscale representation of the radial velocities of the [O II] gas in 3C 34. The positional and kinematical origin is defined by the optical continuum counterpart of the radio galaxy (shown with a cross).

observed [O II]λ3727 luminosity, is then comparable with that of a typical 3CR quasar at a similar redshift.

Although this interpretation can account for the excitation and the overall warm gas morphology, it is insufficient to explain the observed velocity and line-width structures. The simplest photoionization model would assume that the ionization cone is merely illuminating gas clumps, of random velocity, in a typical cluster environment. The primary difficulty with this interpretation is that the line-emission on the eastern side of 3C 34 shows a remarkably flat velocity structure across a length of more than 70 kpc (see Figure 4).

In contrast to the random velocities generally associated with cluster environments, the uniformity across such large scales indicates that a *single* mechanism is required that will act on all of this region simultaneously. We therefore propose that the radio source, through the bulk motions of its lateral expansion, has swept up the gas that existed in the environment of 3C 34. In this way the gas that makes up the eastern [O II] line-emission region is compressed, pushed to the outer edge of the radio lobes, and given a bulk velocity that is constant across the entire region. A close correlation between the line-emitting

gas and the outer edges of the 20 cm radio emission, as well as the radio depolarization associated with the [O II] gas (Johnson et al. 1995), also support this interpretation.

In our photoionization scenario there exists a direct cause and effect relationship between the radio source and the ionization cone that leads to the alignment effect in 3C 34. It is possible to imagine that the nucleus was initially surrounded by a cloud opaque to ionizing radiation in all directions. When the radio jet turned on it plowed through the cloud and opened up a low density channel. As the radio lobes grew in size the increased density of the swept up gas allows it to effectively absorb the incident ionizing radiation from the central AGN which, in turn, can effectively escape along the cleared out, low density channel created by the radio source.

The obvious conical structure in 3C 34, though previously unobserved in high redshift, powerful radio galaxies, is well-known in 11 low redshift Seyferts. The tight alignment between the cone and radio axes found in these sources ($\Delta PA_{mean}=6°$; Wilson & Tsvetanov 1994) is also true for 3C 34. A fundamental difference, however, is that the Seyfert ionization cones show line-emission gas across the entire lateral extent of their opening angles. The fact that 3C 34's radio power is more than four orders of magnitude greater, and hence capable of effectively sweeping out the IGM of the radio galaxy, and confining the line-emitting gas to its edges, is a plausible explanation for this difference.

Class 3: A direct shock interaction with the radio source.

In this model (see Meisenheimer & Hippelein 1992 for a detailed description) the radio jet bowshock sweeps up and heats the ambient medium, thereby compressing and accelerating the gas. The gas which has passed through this shock then requires several 10^7 years before it can sufficiently cool to be visible in optical line-emission. This results in a downstream lag between the [O II] emitting gas and the current position of the radio hotspots of a few tens of kpc. As a natural consequence of the close correlation between the radio source and the warm gas, galaxies dominated by this model tend to be very well-aligned and have the greatest degree of symmetry in their line-emission morphology and kinematics. They are also characterized by having the largest line widths ($\Delta v \gtrsim 1000\,km\,s^{-1}$) of all of our sample sources (*e.g.* **3C 368** and 3C 352). For a number of galaxies we have also proposed a weaker version of this model involving an interaction between the lateral expansion/backflow of the radio lobes and the [O II] gas (*e.g.* 3C 34 and 3C 337).

Noticeably absent from the list of mechanisms for explaining the emission-

line excitation is the popular jet-induced starburst scenario. In this model the radio source propagates through the ambient medium, compresses the gas through its bowshock or overpressure cocoon, and triggers a burst of star formation (*e.g.* McCarthy et al. 1987; DeYoung 1989; Begelman & Cioffi 1989). Using the spectral synthesis models of Bruzual & Charlot (1993), we have computed the spectral energy distribution of a starburst constructed to maximize its output of ionizing radiation. The observed [O II]λ3727 flux constrains the mass of this burst, and allows a prediction of its continuum signature. Since we find the continuum flux underlying the line-emission regions to be non-existent or far too weak in virtually all sources, we can strongly argue against this model.

References

Baum, S. A., Heckman, T. M., Bridle, A. H., van Breugel, W. J. M., & Miley, G. 1988, APJS, 68, 643

Begelman, M. C., & Cioffi, D. F. 1989, APJL, 345, L21

Bruzual, G. A., & Charlot, S. 1993, APJ, 405, 538

Chambers, K. C., Miley, G. K., & van Breugel, W. 1987, *Nature*, 329, 604

DeYoung, D. S. 1989, APJL, 342, L59

Eales, S. A. 1992, APJ, 397, 49

Johnson, R. A., Leahy, J. P., & Garrington, S. T. 1995, MNRAS, 273, 877

McCarthy, P. J., van Breugel, W., Spinrad, H., & Djorgovski, S. 1987, APJL, 321, L29

McCarthy, P. J., Spinrad, H., & van Breugel, W. 1995, APJS, 99, 27

Meisenheimer, K., & Hippelein, H. 1992, A&A, 264, 455

Neeser, M. J., Meisenheimer, K., & Hippelein, H. 1997, APJ, 492

Neeser, M. J., Hippelein, H. & Meisenheimer, K. 1998, APJ, in prep

Neff, S. G., Roberts, L., & Hutchings, J. B. 1995, APJ, 99, 349

Wilson, A. S., & Tsvetanov, Z. I. 1994, AJ, 107, 1227